http://dx.doi.org/10.5012/bkcs.2013.34.10.3005

Effect of Manganese Promotion on Al-Pillared Montmorillonite Supported Cobalt Nanoparticles for Fischer-Tropsch Synthesis

N. Ahmad,[†,‡,#,*] S. T. Hussain,[‡] B. Muhammad,[†] N. Ali,[§] S. M. Abbas,[‡] and Y. Khan[‡]

[†]*Department of Chemistry, Hazara University, Mansehra, 21300, Pakistan.* [*]*E-mail: nisar_shawar@yahoo.com*
[‡]*National Centre for Physics, QAU Campus, Islamabad, 43520, Pakistan*
[§]*Department of Physics, University of the Punjab, Lahore, 54000, Pakistan*
[#]*Department of Environmental Science, University of Swat, Pakistan*
Received February 23, 2013, Accepted July 22, 2013

The effect of Mn-promotion on high surface area Al-pillared montmorillonite (AlMMT) supported Co nanoparticles prepared by hydrothermal method have been investigated. A series of different weight% Mn-promoted Co nanoparticles were prepared and characterized by XRD, TPR, TGA, BET and SEM techniques. An increase in the surface area of MMT is observed with Al-pillaring. Fischer-Tropsch catalytic activity of the as prepared catalysts was studied in a fixed bed micro reactor at 225 °C, $H_2/CO = 2$ and at 1 atm pressure. The data showed that by the addition of Mn the selectivity of C_1 dropped drastically while that of C_2-C_{12} hydrocarbons increased significantly over all the Mn-promoted Co/AlMMT catalysts. The C_{13}-C_{20} hydrocarbons remained almost same for all the catalysts while the selectivity of C_{21+} long chain hydrocarbons decreased considerably with the addition of Mn. The catalyst with 3.5%Mn showed lowest C_{21+} and highest C_2-C_{12} hydrocarbons selectivity due to cracking of long chain hydrocarbons over acidic sites of MMT.

Key Words : Cobalt, Aluminium, Montmorillonite, Manganese promotion, FT Synthesis

Introduction

Due to increasing energy demands and rapidly depleting resources of petroleum, huge reservoir of natural gas, coal and biomass can be utilized as an alternative to crude oil for the synthesis of sulfur, aromatics and nitrogen free ultra clean fuels along with value added fine chemicals *via* Fischer-Tropsch (FT) synthesis.[1,2]

FT synthesis reaction has attracted worldwide attention to convert syngas (CO and H_2) *via* gasification of coal, natural gas and biomass to liquid hydrocarbons by the use of different catalysts.[3,4] The most widely used catalysts for the FT synthesis include different forms of Ni, Fe, Ru and Co metals. The use of these catalysts is limited due to the excessive CH_4 production in case of Ni and high price of Ru, leaving only Co and Fe as feasible catalysts in FT synthesis.[5] Due to the lower extent of deactivation, water gas shift activity and selectivity towards linear hydrocarbons, Co is preferred over Fe-based catalysts in academic as well as on industrial scale.[6]

The catalytic activity of Co-based catalysts can be improved by the dispersion of Co on the surface of refractory oxides such as silica and alumina and mesoporous oxides like MCM-48, MCM-41 and SBA-15 which are thought to be responsible for increase in the surface area of Co and hence its catalytic activity.[6-10] The catalytic activity as well as the products selectivity of FT catalysts is also affected by the nature of support. In FT synthesis, Zeolites have been used as a support to synthesize hydrocarbons of specific molecular weights and to change the FT catalyst products distribution.[11]

The application of montmorillonite (MMT), a naturally occurring layered material has been studied extensively in the field of catalysis for the hydrocracking of petroleum products in refineries.[12] Besides this pillared clay supported Co-catalysts show good selectivity and catalytic activity in FT synthesis.[13] But the presence of alkali metals especially Na in the MMT catalyst is responsible for the production of large amount of CH_4, CO_2 and lower FT catalytic activity, due the hindrance in CoO reduction. The FT catalytic activity of MMT supported catalysts can be increased by pillaring MMT with certain larger metal cations, among which Al show higher CO-conversion, indicating that AlMMT has a positive impact on the CO-conversion in FT synthesis.[4]

The addition of Mn, Ti, Zr *etc.* as a promoter can also boost the performance and suppress the metal support interaction of FT catalysts.[14-20] The CH_4 selectivity of Fe or Co-FT catalysts is significantly decreased by the addition of Mn.[21] It is reported that Mn-promotion stabilizes the catalytic activity, improves the formation of light olefins, higher hydrocarbons and decreases the CH_4 selectivity for Fe, Co-FT catalysts.[22-26] Also the metal support interaction in case of Co/TiO_2-FT catalyst is suppressed by the addition of 3 wt % Mn and the selectivity of this system for lower olefins and C_{5+} hydrocarbons is enhanced due the stabilization of larger Co particles.[26-28] To decrease the methane and increase the hydrocarbons selectivity the promotional effect of Ce or Ru on Co catalysts supported on pillared MMT has also been reported,[13] though there is no report on the effect of Mn on MMT supported Co-catalysts for FT synthesis.

In light of the above discussion, we have set ourselves a task to study the effect of Al-pillaring and the promoter

effect of Mn on AlMMT supported cobalt nanoparticles for FT reaction.

Experimental

Materials. Sodium montmorillonite (NaMMT), Aluminium chloride ($AlCl_3·6H_2O$), manganese nitrate ($Mn(NO_3)_2·4H_2O$) and cobalt nitrate ($Co(NO_3)_2·6H_2O$) from Sigma-Aldrich were of analytical grade and used without any further purification. NaMMT was selected as a starting material to prepare the AlMMT.

Preparation of AlMMT. In a typical synthesis procedure, 0.5 M NaOH solution was slowly added to 0.25 M solution of $AlCl_3·6H_2O$ with OH/Al ratio of 2/1 with continuous stirring. This suspension was aged at room temperature for 24 h. In the second step, above pillaring solution was added (5 mmol Al/g of clay) to the suspension of 2 wt % MMT and stirred for 3 h at 100 °C. The resultant slurry was centrifuged at 5000 rpm, washed several times with deionized water in order to remove excess sodium and chlorine, dried overnight at 100 °C, grinded and finally calcined at 400 °C for 5 h.[29,30]

Preparation of Different wt % Mn-20 wt % Co/AlMMT. 20 wt % Co/AlMMT and 20 wt % Co/AlMMT with 0.10, 0.30, 0.70, 1.50, 3.50 wt % Mn designated as 0.10Mn-Co/AlMMT, 0.30Mn-Co/AlMMT, 0.70Mn-Co/AlMMT, 1.5Mn-Co/AlMMT, 3.5Mn-Co/AlMMT respectively, were synthesized by hydrothermal method.

To prepare 5 g of catalyst, a calculated amount of the calcined pillared clay was added to calculated amount of $Co(NO_3)_2·6H_2O$ and $Mn(NO_3)_2·6H_2O$ (0.1 molar solution) with constant stirring. The resultant suspension along with NH_4OH (33%) was transferred into teflon-lined stainless stell autoclave previously flushed with argon. The pressure of the autoclave was increased from 10 bar to 20 bar on heating at 160 °C for 1 h. After thermal treatment the resultant material was cooled, filtered, washed thoroughly with deionized water to remove all the NH_4OH and then dried overnight at 100 °C. The dried material was grinded & then sieved through a 125 μm sieve and finally calcined at 400 °C for 5 h.

Characterization of Prepared Catalysts. The synthesized catalysts were analyzed using Scintag XDS 2000 diffractometer. BET surface area and pore volume were measured at liquid nitrogen temperature (78 K) by Coulter SA 3100 BET surface area and pore volume analyzer. The reduction study for supported cobalt phase was carried out using H_2-Temperature Program Reduction Catalytic Surface Analyzer (TPDRO/1100 Series, Thermo Electron Corporation, Italy). Thermo gravimetric analysis (TGA) of all catalysts has been studied on Mettler TGA/SDTA 851e. The morphological and compositional characterization of catalysts were carried out with scanning electron microscopy (JEOL JSM 6490-A) equipped with Energy Dispersive X-ray Spectrometer (EDX).

Catalyst Evaluations. The catalytic test was carried out in a fixed bed micro reactor Figure 1 operating at atmospheric pressure. Different experiments with catalyst volume, reaction temperature, reaction pressure and composition were performed and tested for activity and selectivity. From this data, experimental conditions were standardized. The Mn-promoted Co/AlMMT catalyst (1.0 g) was held in the middle of the reactor using quartz wool. It was pre-reduced in situ at atmospheric pressure in a flowing H_2 stream at 400 °C for 6 h before syngas exposure. The H_2/CO reaction was carried out at 225 °C (P = 1 atm, H_2/CO = 2) for 30 h. Reactant and product streams were analyzed using on line gas chromatograph (Varian, model CP-3800) equipped with a sample loop, a thermal conductivity detector and flame ionization detector. The contents of sample loop were injected automatically into a packed column (CP-PoraPLOT Q fused silica PLOT, 25 m × 0.53 mm, dn = 20 μm). Helium was employed as a carrier gas for optimum sensitivity. The calibration of GC was carried out using standerd hydrocarbons mixtures and pure compounds obtained from Scott Specialty Gases, UK.[31]

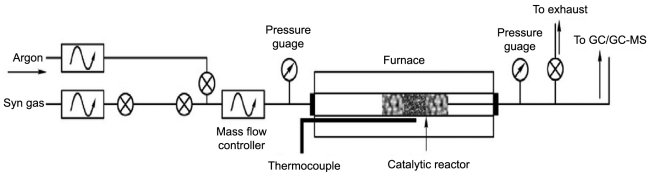

Figure 1. Schematic diagram showing the positioning of equipment and flow of gases.

Results and Discussion

Textural and Structural Properties. Figure 2(a) shows the XRD pattern of MMT having (001) diffraction peak with a basal spacing of 12.06 Å and the thickness of the host layer of MMT is 9.3 Å.[30] The gallery height was found to be 3.3 Å, which was calculated by subtracting the host layer thickness from the basal spacing of the MMT.

As can be observed in the XRD pattern of AlMMT in Figure 2(b), the Al-addition has shifted the peak to a lower 2θ value with a corresponding increase in d-spacing from 12.06 to 18.7 Å and the gallery height from 3.3 to 9.4 Å. This causes the expansion of the clay inter planar distance with Al-pillar, similar to the ionic structure of Keggin type

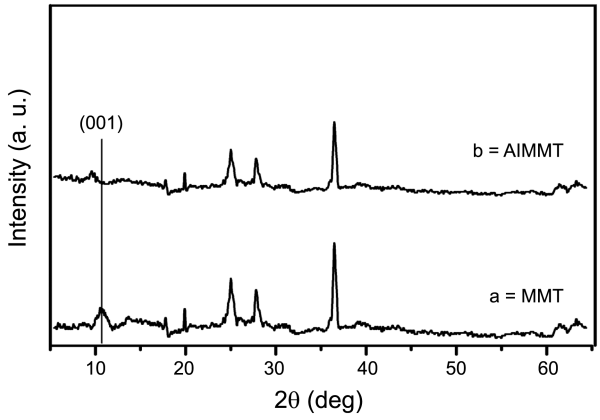

Figure 2. XRD pattern of (a) MMT (b) AlMMT.

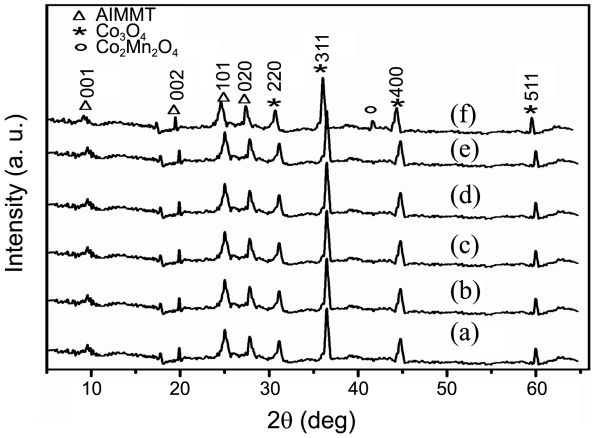

Figure 3. XRD pattern of (a) Co/AlMMT (b) 0.10Mn-Co/AlMMT (c) 0.30Mn-Co/AlMMT (d) 0.70Mn-Co/AlMMT (e) 1.5Mn-Co/AlMMT (f) 3.5Mn-Co/AlMMT.

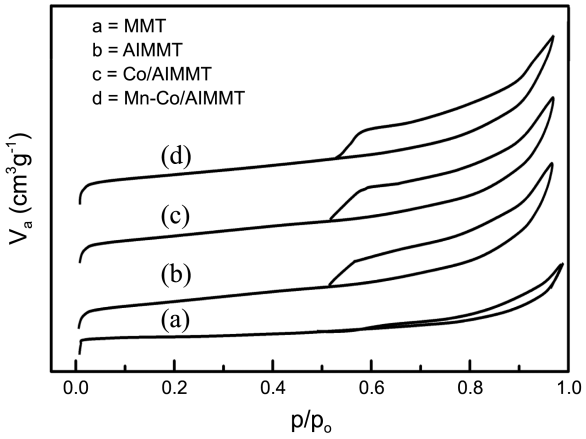

Figure 4. Adsorption desorption isotherm of MMT, AlMMT, Co/AlMMT and Mn-promoted Co/AlMMT.

$[Al_{13}O_4(OH)_{24}(H_2O)_{12}]^{7+}$ as reported in reference.[12,29,32] The intensity of the (001) peak was also decreased which can be attributed to the intercalation of Al into the MMT clay interlayer's, no other structural changes were observed in the XRD spectra of both the samples as rest of the peak positions remained unchanged.

Figure 3 shows the XRD pattern of AlMMT catalysts loaded with Mn and Co. All the catalysts show (001) diffraction peaks and basal reflection of AlMMT with a small decrease in their intensity which corresponds to the slight decrease in layered structure of MMT. Co-loaded catalysts giving cubic cobalt oxides (Co_3O_4) diffraction at 19.1°, 31.4°, 37°, 45° and 60° (JCPDS 65-3103) indicated a uniform dispersion of pure Co_3O_4 nanoparticles on pillared MMT.

The average crystallite size of the Co_3O_4 nanoparticles calculated using the scherer equation was found to be in the range of 22-50 nm. Due to high dispersion and lower content of Mn on AlMMT, all the XRD spectra showed no peaks corresponding to Mn or $Co_{3-x}Mn_xO_4$ with the exception of 3.5Mn-Co/AlMMT as shown in Figure 3(f), which showed a small peak for $Co_{3-x}Mn_xO_4$ and a shift to lower 2θ value as observed in another study.[28] There was no reflection of cobalt aluminates or silicate in the XRD pattern confirming that only highly dispersed Co_3O_4 phase exists. The addition of Mn helped in uniform dispersion of Co_3O_4 nanoparticles and enhanced the reduction responsible for increased FT activity.

Figure 4 shows the N_2 adsorption and desorption isotherm of Mn-promoted Co/AlMMT which is Type IV isotherm indicative of porous structure of AlMMT. The narrow slit shaped porous structure of MMT was confirmed after Al pillaring from the hysteresis loop. The Mn and Co-loading to the AlMMT did not change its narrow slit shape porous structure as obvious from the same isotherm shown for all the catalysts, although there was a decrease in the BET surface area for Co and Mn-loaded Al-pillared catalysts along with minor changes in pore diameter and volume.

Table 1 shows BET surface area, pore diameter and average pore volume of our prepared catalysts after calcinations at 400 °C. There was no evidence of decrease in surface area for all prepared catalysts upon calcinations at 400 °C.

The pillaring of MMT with Al produces significant increase in the surface area from 39.243 to 254 m^2/g along with increase in pore volume and pore diameter, which can be explained by the contribution of Al to replace the Na^+ in the MMT causing its pore openings to adsorb N_2.[12] The loading of Co nanoparticles and Mn to the catalysts produce minor decrease in the surface area, pore diameter and pore volume of AlMMT which may be attributed to the presence of active metal particle on the surface and specifically at pore openings but the average pore size and volume remains constant for all of the catalysts, therefore the pore blocking of Co and Mn are negligible.[13] The total pore diameter of our prepared catalysts AlMMT, Co/AlMMT, and Mn-promoted Co/AlMMT were 18.3 Å, 15.75 Å and 17.32 Å which are larger than the inter layer distance of these catalysts. The reason for this increase in pore size is the formation of delaminated structure responsible for increase in MMT pore size, a similar behavior reported in reference.[30] Due to the larger BET surface area 254 m^2/g and much larger pore size, we claim that AlMMT can play a positive role as support for the FT catalysts.

SEM Studies. SEM characterization was carried out to study the surface morphology of prepared catalysts. Powdered specimens of the samples were used to obtain SEM micrograph. The SEM micrograph in Figure 5(c) and (d) showed uniform distribution of Co nanoparticles on the surface of AlMMT, pillaring with Al, loading of Co and Mn to the MMT and calcinations at 400 °C produced no distinct

Table 1. Textural properties of the prepared catalysts

Sample	BET (m^2/g)	Pore diameter (Å)	Pore volume (cm^3/g)
MMT	39.2	4.8	0.08
AlMMT	254.0	14.6	0.20
Co/AlMMT	235.0	15.75	0.189
Mn-promoted Co/AlMMT	229.68	17.32	0.19

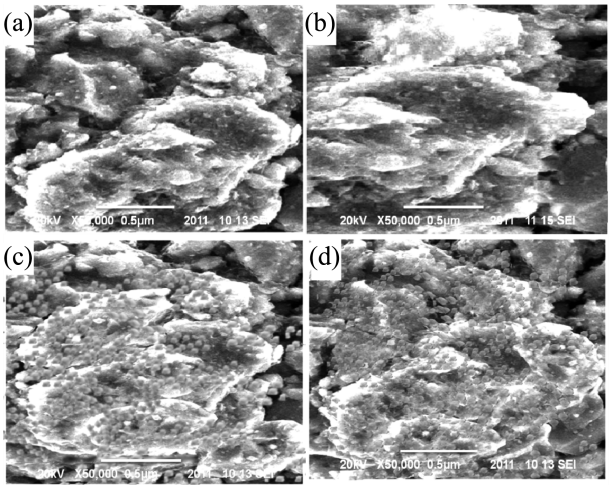

Figure 5. SEM Images of (a) MMT (b) AlMMT (c) Co/AlMMT (d) Mn-promoted Co/AlMMT.

effect on the layered structure of MMT, hence the flake like morphology of MMT remained unchanged.

Reduction Behavior. Figure 6 shows the reduction profile of as prepared catalysts. The reduction of cobalt oxide normally takes place in two steps.

$$\text{(i) } Co_3O_4 \rightarrow CoO \quad (1)$$

$$\text{(ii) } CoO \rightarrow Co^o \quad (2)$$

The Co/AlMMT catalyst showed two reduction peaks at 268 °C and 365 °C for Eqs. (1) and (2), respectively. A distinct change in the TPR profile was observed for Mn-promoted Co/AlMMT catalyst. The reduction of Co_3O_4 occurs at different temperatures for different wt % of Mn as shown in Table 2.

A decrease in reduction temperature was observed for a lower Mn-loading up to 0.70% for both reactions in Eqs. (1) and (2) while for 1.5% a decrease in the reduction temperature for reactions in Eq. (2), because of high degree of dispersion and stabilization of Co_3O_4.

The highest Mn-loading (3.5%wt) hindered the reduction of Co_3O_4 possibly due to the formation of Co-Mn spinal or mixed Co-Mn oxides on the surface. The high temperature

Table 2. Two steps Co_3O_4 reduction Temperature

Catalysts	Reduction Temperature	Reduction Steps
0.10Mn-Co/AlMMT	265 °C	Eq. (1)
	350 °C	Eq. (2)
0.30Mn-Co/AlMMT	255 °C	Eq. (1)
	335 °C	Eq. (2)
0.70Mn-Co/AlMMT	270 °C	Eq. (1)
	345 °C	Eq. (2)
1.5Mn-Co/AlMMT	300 °C	Eq. (1)
	368 °C	Eq. (2)
3.5Mn-Co/AlMMT	395 °C	Eq. (1)
	595 °C	Eq. (2)

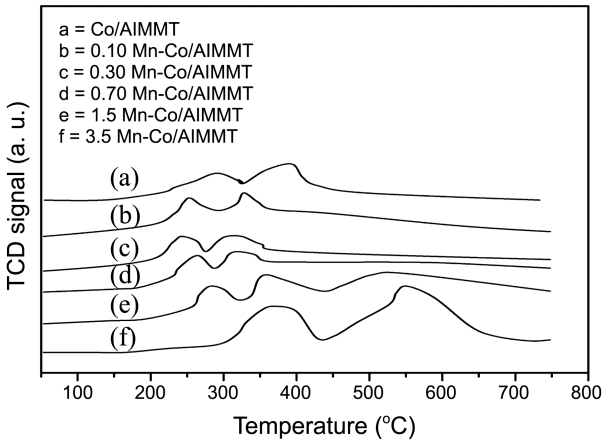

Figure 6. H_2 TPR profile of the prepared samples.

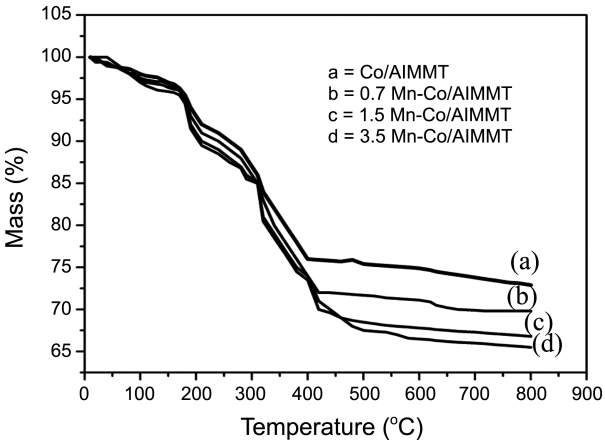

Figure 7. TGA of Co/AlMMT and Mn-promoted Co/AlMMT.

reduction peak at 595 °C in the TPR profile of 3.5% Mn was assigned to Co-Mn spinal reduction as reported in the previous findings.[28] It can thus be inferred that the minimum loading of Mn enhances and promotes the Co_3O_4 reduction, which becomes less significant as we increase the Mn-loading.

Thermogravimetric Analysis (TGA). To study the decomposition of our prepared catalysts at high temperature thermo gravimetric analysis (TGA) was performed as shown in Figure 7. TGA spectra showed that Co/AlMMT and Mn-promoted Co/AlMMT follow continuous weight loss till 800 °C. Weight loss at 160 °C can be attributed to the evaporation of adsorbed water on the surface of the sample,[33-36] while the continuous weight loss from 160 °C to 800 °C with variation at 400 °C was attributable to the removal of hydroxide groups as a result of dehydroxylation of pillar and clay structure, causing collapse in MMT layer structure.[37] The increased Mn-loaded samples showed greater weight loss due to the dehydroxylation of Co and Mn species, which is in agreement with the previous reported data for Vanadia-loaded pillared clays.[33]

FT Catalytic Performance

Effect of Mn-addition on Co-based FT Catalysts. Several

reports on the effect of Mn addition on the catalytic activity of Co supported on several supports. Silicalite-1 supported Co-Mn catalyst was reported by Das *et al.*.[38] Due to the addition of Mn, good activity and selectivity for light hydrocarbons in the C_2-C_4 range was attained along with very low WGS activity. Moreover, the addition of Mn increased the CO conversion while the selectivity towards alkenes slightly decreased. ZSM-5 supported Mn-Co FT catalyst was investigated by Koh *et al.*.[39] The results showed that the Mn promoted ZSM-5 supported catalyst resulted in the cracking of high molecular weight hydrocarbons into lower alkanes. Zhang *et al.* reported the Mn-promotion in Co/Al_2O_3 catalysts.[40] It was observed that Mn improved the catalytic activity in addition to the C_{5+} selectivity. On the other hand methane formation and C_{2-4} hydrocarbons was considerably reduced. Mn-promoted Co/SiO_2 catalyst was investigated by Klabunde *et al.*.[41] The high CO conversion and C_{5+} hydrocarbon selectivity was achieved due to increased Co dispersion. Voβ *et al.* reported the effects of Mn-promoter on Co/TiO_2 catalysts.[42] It was concluded that MnO had little effect on the catalytic properties and worked only as an additional support. The use of mesoporous Co/SBA-15 catalysts promoted with Mn for FT synthesis was studied by Martinez *et al.*.[43] Mn enhanced the formation of *n*-paraffins (C_{10+}), while decrease in methane selectivity was observed. The use of Mn-promoted MMT supported Co based FT catalyst have been investigated for the first time in this study.

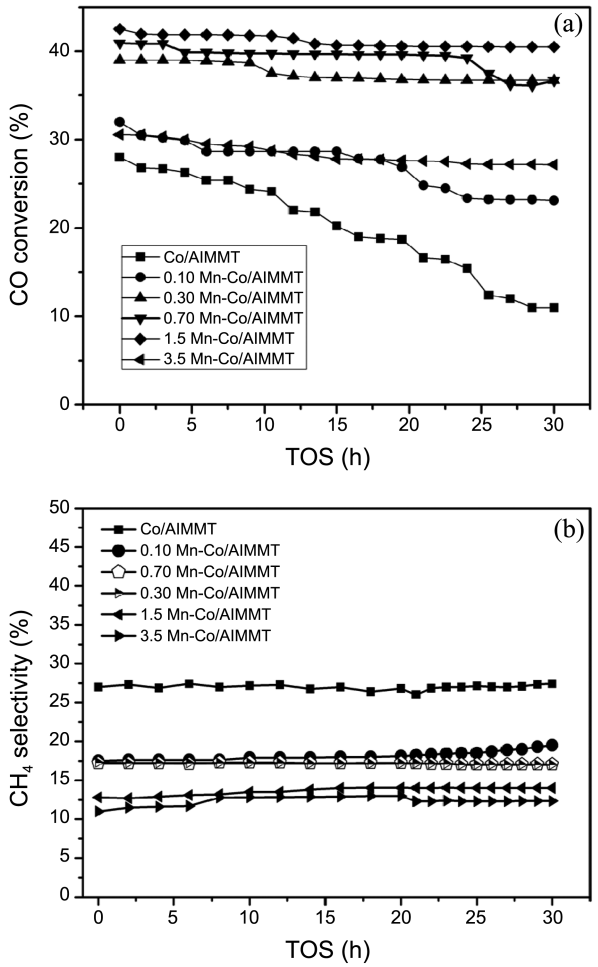

Figure 8. (a) CO-conversion (b) CH_4 Selectivity Vs Time on stream over Co/AlMMT and Mn-promoted Co/AlMMT catalysts.

The catalytic performance of Co/AlMMT and Mn-promoted Co/AlMMT in terms of CO-conversion, CH_4 selectivity and time on stream is presented in Figure 8(a), (b) respectively.

One of the main disadvantage of the AlMMT supported catalyst is its higher selectivity towards CH_4, which is the most undesirable product of FT synthesis due its behavior of cracking reaction.[44] For this reason, the catalysts were promoted with Mn and the effects of Mn-promotion is shown in Figure 8(a), (b). The CO-conversion (%) is calculated according to the normalization method given below.[22,31]

$$\text{CO-Conversion (\%)} = \frac{(\text{Moles of CO}_{in}) - (\text{Moles of CO}_{out})}{\text{Moles of CO}_{in}} \times 100$$

The selectivity (%) towards the individual components on carbon-basis is calculated according to the same principle:

$$\text{Selectivity of J product (\%)} = \frac{\text{Moles of J product}}{(\text{Moles of CO}_{in}) - (\text{Moles of CO}_{out})} \times 100$$

CO-Conversion. 20 wt % Co/AlMMT catalysts showed higher CO-conversion of up to 28% (Figure 8(a)) which decreased with time on stream (TOS) and reached a minimum of 11% after 10 h of TOS. The CO-conversion increased to around 42% for an initial increase in the Mn-loading of upto 1.5 wt % but further loading of Mn (3.5 wt %) resulted in a reduced CO-conversion of up to 30% which is nearly equal to that for Co/AlMMT catalyst. Since the FT reaction occurred on the surface of metallic cobalt rather than oxide of cobalt, therefore, the catalytic activity and selectivity was largely dependent upon the reduction of Co_3O_4 to metallic Co. The lowered catalytic activity and higher CH_4 selectivity Co/AlMMT catalysts was due to the incomplete reduction of Co_3O_4 near the reaction temperature. Thus increased catalytic activity and lower CH_4 selectivity (Figure 8(b)) were achieved by Mn-promotion obvious from the H_2-TPR profile (Figure 6) that Mn-loading helped to lower the reduction temperature of Co_3O_4, as a result of small and highly dispersed Co particles formation as compared to the un promoted Co_3O_4. While the decreased activity of high Mn-loading (3.5 wt %) as shown in Figure 8(b), was due to the hindered reducibility of Co_3O_4 as evident from the H_2-TPR profile shown in Figure 6. The highest Mn-loading (3.5 wt %) hindered the reduction of Co_3O_4 possibly due to the formation of Co-Mn spinal or mixed Co-Mn oxides on the surface, hence their catalytic activity is decreased.

Apart from this, the Mn-addition to the Co/AlMMT catalyst increased the catalyst stability, as the catalysts having larger Mn-loading showed greater TOS stability and is in

Table 3. Results of different catalysts for FT synthesis

Catalysts	CO conversion	CO_2 Selectivity	C_1 (wt %)	C_2-C_{12} (wt %)	C_{13}-C_{20} (wt %)	C_{21} (wt %)
Co/NaMMT	10.0	2.3	40.0	12.5	8.0	37.2
Co/AlMMT	28.0	2.5	27.2	18.2	11.0	41.0
0.10Mn-Co/AlMMT	32.0	2.6	19.5	38.8	9.3	29.3
0.30Mn-Co/AlMMT	39.0	2.4	17.0	31.9	12.0	36.3
0.70Mn-Co/AlMMT	40.9	2.5	17.0	39.5	13.0	26.5
1.5Mn-Co/AlMMT	42.5	2.6	14.0	44.0	11.0	28.4
3.5Mn-Co/AlMMT	30.5	2.6	12.98	63.0	4.0	17.2

agreement with previously reported data.[45]

CH_4 Selectivity. Figure 8(b) shows the CH_4 selectivity of the prepared catalysts with TOS. The Co/AlMMT catalyst showed higher CH_4 selectivity of 27% which remained constant on TOS for 30 h. For the Mn-promoted Co/AlMMT catalyst, the CH_4 selectivity decreased with increase of Mn-content along with increase in CO-conversion for Co/AlMMT catalyst.[28] The CH_4 selectivity for 0.10Mn-Co/AlMMT, 0.30Mn-Co/AlMMT, 0.70Mn-Co/AlMMT, 1.5Mn-Co/AlMMT, 3.5Mn-Co/AlMMT samples was 19.5%, 17.05%, 17.5%, 17%, 14.1% and 12.5%, respectively which was much lower than that for Co/AlMMT catalyst. The best results showing the least CH_4 selectivity were achieved for 3.5% Mn-loading where a constant 12.5% CH_4 selectivity was observed for 30 h of TOS. This was also observed in another study where lower CH_4, higher olefins and C_5-C_{12} hydrocarbons selectivity of Mn-promoted catalysts was attributed to the presence of large number of Mn atoms on the catalysts surface.[46]

Furthermore, the addition of small quantity of Mn decreased the CH_4 and increased the higher hydrocarbons selectivity due to the electronic effect of Mn which increases the electron density of chemisorptions site of catalysts. This depresses the hydrogen chemisorptions which normally donates electron density to the metal chemisorptions sites, consequently decreasing the coverage of metal surface by hydrogen which is responsible for CH_4 formation. This inhibits CO hydrogenation to CH_4, giving rise to more unsaturated hydrocarbons and enhanced hydrocarbons chain growth as reported in our previous study.[47]

FT Reaction Products of 20 wt % Co-Mn/AlMMT. Al pillaring of MMT resulted in an increase in the surface area of MMT from 39.243 to 254 m^2/g and frequently increase in its catalytic activity.[12] The products obtained over Co/AlMMT catalyst mainly consisted of C_2-C_{12} hydrocarbons and lower concentration of higher molecular weight hydrocarbons C_{21} mainly due to the cracking of long chain hydrocarbons at the acidic site of MMT.[48-52] Since the best results for all the prepared catalysts were obtained for TOS of 8 h, the combined data of the selectivity of the un-promoted and Mn-promoted catalysts at this TOS is presented in Table 3. From this table we find that the selectivity towards C_1, C_2-C_{12}, C_{13}-C_{20} and C_{21} hydrocarbons changed with the addition of small amount of Mn. Acidic sites of MMT catalysts are responsible for the cracking of higher hydrocarbons to increase C_2-C_{12} and decrease C_{21} hydrocarbons selectivity of Mn-promoted Co/AlMMT catalysts. By the addition of Mn the selectivity of C_1 dropped drastically while that of C_2-C_{12} hydrocarbons increased significantly over all the Mn-promoted Co/AlMMT catalysts which was due to the limited hydrogen adsorbed on the surface of catalysts or due to the α olefins re-adsorption by a secondary reaction responsible for chain growth. These findings are in agreement with the results reported by Weckhuysen *et al.* for Mn-promoted catalysts.[26,28] This effect can also be attributed to the Mn and Co interaction.[24,26,45,53,54] Furthermore, the C_{13}-C_{20} hydrocarbons remained almost same for all the catalysts while the selectivity of C_{21+} long chain hydrocarbons decreased considerably with the addition of Mn. The catalysts having 3.5% Mn showed lowest C_{21+} and highest C_2-C_{12} hydrocarbons selectivity. The noticeable improvement in selectivity of C_2-C_{12} hydrocarbons and considerable decrease in selectivity of C_{21+} hydrocarbons can be explained on the basis of cracking of long chain hydrocarbons over MMT based catalysts as reported by Wang *et al.* for Co/ion-exchanged MMT catalysts.[12] In this study, the spillover of hydrogen from Co to the acidic sites was attributed to the long distances between Co present on the surface of MMT and acidic sites of the MMT originated from interlayer region and sheets. This is responsible for increased selectivity of C_2-C_{12} and decreased selectivity of C_{21+} hydrocarbons. These findings are in conformity of the results presented in this study.

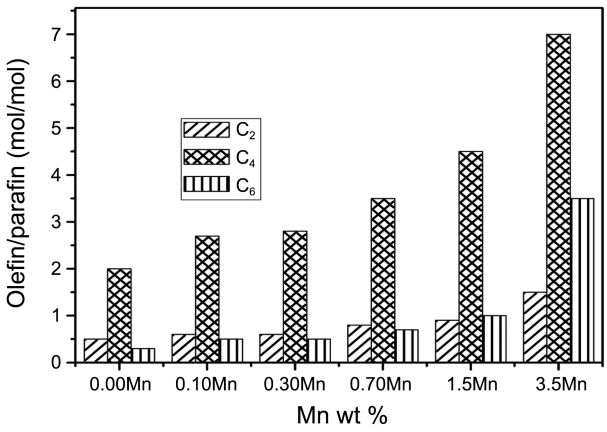

Figure 9. Influence of Mn-promotion on O/P ratio with in C_2-C_6 fraction.

The olefin to paraffin ratio of FT reaction products are shown in Figure 9. It is known that the interaction of Mn with Co decreased the availability of adsorbed hydrogen hence the Mn-promotion increased the olefin to paraffin ratio (O/P).[55] The promotion of catalyst with Mn suppressed the H_2 addition and enhanced the light olefin production as reported previously. [28]

The Co/AlMMT catalyst showed that the C_2-C_4 hydrocarbons were almost olefinic with lower CO-conversion. When the CO-conversion increased, the fraction of C_2-C_4 paraffins also increased and resultantly, olefinic fractions decreased due to the secondary hydrogenation of olefins to paraffins and higher hydrocarbons which had also been reported earlier by Dinse *et al*..[55]

Conclusions

The FT catalytic activity of Co/AlMMT and the effect of Mn-promotion on their activity were investigated in this work. Following are the main conclusions of this study.

(1) The AlMMT having large surface area of 254 m^2/g along with increase in pore volume and pore diameter were valuable support for FT catalysts.

(2) Pillaring with Al, loading of Co and Mn to the MMT and calcinations at 400 ºC had no distinct effect on the layered structure of MMT. The flake like morphology of MMT remains unchanged.

(3) The lower Mn-loading pf upto 1.5% enhanced the reduction of Co_3O_4, which is the most important step in FT synthesis because of high degree of dispersion and stabilization of Co_3O_4.

(4) The catalytic activity of MMT was increased by pillaring with Al and the promotion of catalysts with Mn decreased the CH_4 selectivity and increased the catalytic activity in order of 1.5Mn-Co/AlMMT > 0.7Mn-Co/AlMMT > 0.3Mn-Co/AlMMT > 0.10Mn-Co/AlMMT > 3.5Mn-Co/AlMMT > Co/AlMMT, mainly due to the reduction behavior for all sets of the catalysts.

(5) Mn-promoted Co/AlMMT catalyst showed increased C_2-C_{12} (63.02%) and decreased C_{21+} (20%) hydrocarbons selectivity due to the acidic sites of MMT catalysts which s were responsible for the cracking of higher hydrocarbons.

(6) By the addition of Mn the selectivity of C_1 dropped drastically while that of C_2-C_{12} hydrocarbons increased significantly over all the Mn-promoted Co/AlMMT catalysts.

(7) The promotion of catalyst with Mn suppressed the H_2-addition and enhanced the light olefin production and also increased the olefin to paraffin ratio (O/P).

Further studies on the effect of reaction conditions such as pressure, temperature, and the reactant gas flow rate are underway.

Acknowledgments. The author would like to thank Higher Education Commission of Pakistan for the financial support of this work under Indigenous -5000 PhD Fellowship program. And the publication cost of this paper was supported by the Korean Chemical Society.

References

1. Dry, M. E. *Catal. Today* **2002**, *71*, 227.
2. Khodakov, A. Y.; Chu, W.; Fongarland, P. *Chem. Rev.* **2007**, *107*, 1692.
3. Schulz, H. *Appl. Catal. A* **1999**, *186*, 3.
4. Font Freide, J. J. H. M.; Gamlin, T. D.; Graham, C.; Hensman, J. R.; Nay, B.; Sharp, C. *Top. Catal.* **2003**, *26*, 3.
5. Li, S.; Krishnamoorthy, S.; Li, A.; Meitzner, G. D.; Iglesia, E. *J. Catal.* **2002**, *206*, 202.
6. Jacobs, G.; Das, T. K.; Zhang, Y.; Li, J.; Racoillet, G.; Davis, B. H. *Appl. Catal. A* **2002**, *233*, 263.
7. Li, H.; Wang, S.; Ling, F.; Li, J. *J. Mol. Catal. A: Chem.* **2006**, *244*, 33.
8. Panpranot, J.; Goodwin, J. G., Jr; Sayari, A. *J. Catal.* **2002**, *211*, 530.
9. Xiong, H.; Zhang, Y.; Liew, K.; Li, J. *J. Mol. Catal. A: Chem.* **2008**, *295*, 68.
10. Prieto, G.; Martínez, A.; Murciano, R.; Arribas, M. A. *Appl. Catal. A* **2009**, *367*, 146.
11. Hussain, S. T.; Mazhar, M.; Nadeem, M. A. *J. Nat. Gas Chem.* **2009**, *18*, 187.
12. Wang, G.-W.; Hao, Q.-Q.; Liu, Z.-T.; Liu, Z.-W. *Appl. Catal. A* **2011**, *405*, 45.
13. Su, H.; Zeng, S.; Dong, H.; Du, Y.; Zhang, Y.; Hu, R. *Appl. Clay Sci.* **2009**, *46*, 325.
14. Zhang, Y.; Shinoda, M.; Tsubaki, N. *Catal. Today* **2004**, *93-95*, 55.
15. Shinoda, M.; Zhang, Y.; Yoneyama, Y.; Hasegawa, K.; Tsubaki, N. *Fuel Process. Technol.* **2004**, *86*, 73.
16. Wei, M.; Okabe, K.; Arakawa, H.; Teraoka, Y. *Catal. Commun.* **2004**, *5*, 597.
17. Hinchiranan, S.; Zhang, Y.; Nagamori, S.; Vitidsant, T.; Tsubaki, N. *Fuel Process. Technol.* **2008**, *89*, 455.
18. Nurunnabi, M.; Murata, K.; Okabe, K.; Inaba, M.; Takahara, I. *Appl. Catal. A* **2008**, *340*, 203.
19. Nurunnabi, M.; Murata, K.; Okabe, K.; Inaba, M.; Takahara, I. *Catal. Commun.* **2007**, *8*, 1531.
20. Liu, Y.; Hanaoka, T.; Murata, K.; Okabe, K.; Takahara, I.; Sakanishi, K. *React. Kinet. Catal. L* **2007**, *92*, 147.
21. Hindermann, J. P.; Hutchings, G. J.; Kiennemann, A. *Catal. Rev.* **1993**, *35*, 1.
22. Mirzaei, A. A.; Faizi, M.; Habibpour, R. *Appl. Catal. A* **2006**, *306*, 98.
23. van der Riet, M.; Copperthwaite, R. G.; Hutchings, G. J. *J. Chem. Soc., Faraday Trans. 1 F: Phy. Chem. Condensce Phas.* **1987**, *83*, 2963.
24. Bezemer, G. L.; Radstake, P. B.; Falke, U.; Oosterbeek, H.; Kuipers, H. P. C. E.; van Dillen, A. J.; de Jong, K. P. *J. Catal.* **2006**, *237*, 152.
25. van der Riet, M.; Hutchings, G. J.; Copperthwaite, R. G. *J. Chem. Soc., Chem. Commun.* **1986**, 798.
26. Morales, F.; de Smit, E.; de Groot, F. M. F.; Visser, T.; Weckhuysen, B. M. *J. Catal.* **2007**, *246*, 91.
27. Morales, F.; Grandjean, D.; Mens, A.; de Groot, F. M. F.; Weckhuysen, B. M. *J. Phys. Chem. B* **2006**, *110*, 8626.
28. Feltes, T. E.; Espinosa-Alonso, L.; Smit, E. D.; D'Souza, L.; Meyer, R. J.; Weckhuysen, B. M.; Regalbuto, J. R. *J. Catal.* **2010**, *270*, 95.
29. Martinez, M. J.; Fetter, G.; Domunguez, J. M.; Melo-Banda, J. A.; Ramos-Gomez, R. *Microporous and Mesoporous Mater.* **2003**, *58*, 73.
30. Liu, Y.; Murata, K.; Okabe, K.; Inaba, M.; Takahara, I.; Hanaoka, T.; Sakanishi, K. *Top. Catal.* **2009**, *52*, 597.
31. Hussain, S. T.; Ahmad, N.; Muhammad, B. *Current. Catal.* **2012**, *1*, 24.
32. Bineesh, K. V.; Kim, M.-I.; Lee, G.-H.; Selvaraj, M.; Park, D.-W. *Appl. Clay Sci.* **2012**, *74*, 127.
33. Bineesh, K. V.; Kim, D.-K.; Kim, D.-W.; Cho, H.-J.; Park, D.-W. *Energy. Environ. Sci.* **2010**, *3*, 302.

34. Bineesh, K. V.; Kim, S.-Y.; Jermy, B. R.; Park, D.-W. *J. Ind. Eng. Chem.* **2009**, *15*, 207.
35. Bineesh, K. V.; Kim, D.-K.; Kim, M.-I. L.; Park, D.-W. *Appl. Clay Sci.* **2011**, *53*, 204.
36. Cañizares, P.; Valverde, J. L.; Sun Kou, M. R.; Molina, C. B. *Microporous and Mesoporous Mater.* **1999**, *29*, 267.
37. Bineesh, K. V.; Kim, D.-K.; Cho, H.-J.; Park, D.-W. *J. Ind. Eng. Chem.* **2010**, *16*, 593.
38. Das, D.; Ravichandran, G.; Chakrabarty, D. K. *Catal. Today* **1997**, *36*, 285.
39. Koh, D. J.; Chung, J. S.; Kim, Y. G. *Ind. & Eng. Chem. Res.* **1995**, *34*, 1969.
40. Zhang, J.-L.; Ren, J.; Chen, J.-G.; Sun, Y.-H. *Acta Phys-Chim Sin.* **2002**, *18*, 260.
41. Tan, B. J.; Klabunde, K. J.; Tanaka, T.; Kanai, H.; Yoshida, S. *J. Am. Chem. Soc.* **1988**, *110*, 5951.
42. Voβ, M.; Borgmann, D.; Wedler, G. *J. Catal.* **2002**, *212*, 10.
43. Martínez, A. N.; López, C.; Márquez, F.; Díaz, I. *J. Catal.* **2003**, *220*, 486.
44. Akhmedov, V. M.; Al-Khowaiter, S. H. *Catal. Rev.* **2007**, *49*, 33.
45. Colley, S.; Copperthwaite, R. G.; Hutchings, G. J.; Van der Riet, M. *Ind. & Eng. Chem. Res.* **1988**, *27*, 1339.
46. Wang, H.; Yang, Y.; Xu, J.; Wang, H.; Ding, M.; Li, Y. *J. Mol. Catal. A. Chemicl*. **2010**, *326*, 29.
47. Hussain, S. T.; Larachi, F. *Journal of Trace and Microprobe Techniques* **2002**, *20*, 197.
48. Kang, S.-H.; Ryu, J.-H.; Kim, J.-H.; Sai Prasad, P. S.; Bae, J. W.; Cheon, J.-Y.; Jun, K.-W. *Catal. Lett.* **2011**, *141*, 1464.
49. Ngamcharussrivichai, C.; Imyim, A.; Li, X.; Fujimoto, K. *Ind. Eng. Chem. Res.* **2007**, *46*, 6883.
50. Dalai, A. K.; Davis, B. H. *Appl. Catal. A* **2008**, *348*, 1.
51. Bao, J.; He, J.; Zhang, Y.; Yoneyama, Y.; Tsubaki, N. *Angewandte Chemie International Edition* **2008**, *47*, 353.
52. Liu, Z. W.; Li, X. H.; Asami, K.; Fujimoto, K. *Catal. Today* **2005**, *104*, 41.
53. Das, D.; Ravichandran, G.; Chakrabarty, D. K. *Appl. Catal. A* **1995**, *131*, 335.
54. Copperthwaite, R. G.; Hutchings, G. J.; Van der Riet, M.; Woodhouse, J. *Ind. & Eng. Chem. Res.* **1987**, *26*, 869.
55. Dinse, A.; Aigner, M.; Ulbrich, M.; Johnson, G. R.; Bell, A. T. *J. Catal.* **2012**, *288*, 104.